The method of controlled directional reception

Chuck Sword

INTRODUCTION

Controlled directional reception has been developed over a period of many years in the Soviet Union as a means of processing seismic data. It is based on the work of an American, Rieber (1936), but has been extensively developed in the Soviet Union under the leadership of Dr. L.A. Riabinkin of the Gubkin Institute of Petrochemical and Gas Production in Moscow (Riabinkin, et al., 1962). It was recently described, more or less incorrectly, by Sword (1981), and a specialized version has been described in an article by B.R. Zavalishin that was translated (with some errors) by Sword (Zavalishin, 1982).

During my recent nine-month stay at the Gubkin Institute I had the opportunity to study this method in more detail (I was interested in applying CDR, as it is known, to the processing of converted-wave data), and I will attempt in this article to describe one variant of it.

Several variants of CDR have been developed over the years; the one that I will describe has been designed to work with the densely-sampled multifold data that has become common in recent decades. It is, in many ways, a form of migration before stack, and because this migration can be accomplished extremely quickly, there is some promise that it would be of use in interactively interpreting and migrating data from geologically complex areas.

I will explain in this paper how the CDR method can be used to produce a seismic section when velocity is already known, and how CDR can be used to determine the velocity when it is not known. I will discuss some problems that arise when velocity cannot be assumed to be constant, and will present the results of using the CDR method to process some synthetic data.

NOTATION

It is useful to begin by establishing a consistent system of notation. Figure 1 shows a typical recording geometry.

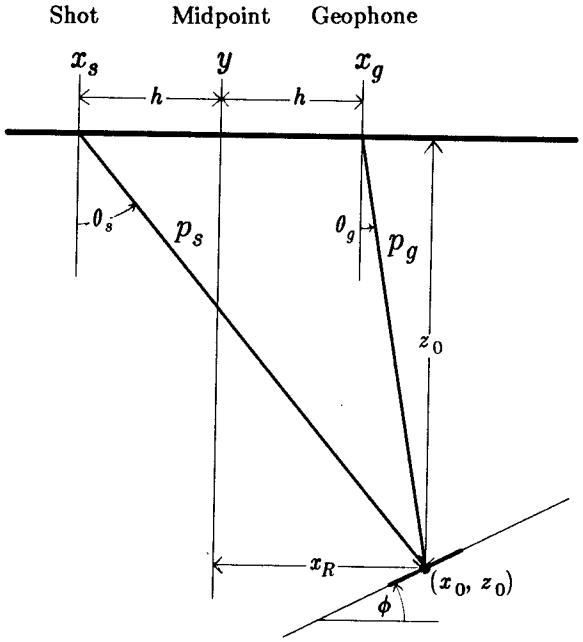

FIG. 1. Typical recording geometry. The figure is drawn so that all parameters shown on it are positive.

The notation used is:

x_s	– Shot position
x_g	– Geophone position
h	– Half offset: $(x_g - x_s)/2$
y	– Midpoint: $(x_g + x_s)/2$
x_0, z_0	– Reflector position
x_R	– Horizontal distance from midpoint y to the reflector.
t	– Travel time
$\overline{v}$	– Average velocity
p_s	– Ray parameter of the downgoing ray ($p_s = -dt/dx_s$)
p_g	– Ray parameter of the upcoming ray ($p_g = -dt/dx_g$)
θ_s	– Angle (from vertical) of the downgoing ray
θ_g	– Angle (from vertical) of the upcoming ray
ϕ	– Angle (from horizontal) of the reflector

In Figure 1 the raypaths have been drawn as straight lines, even though $\overline{v}$ is defined as an average velocity, implying that velocity is not necessarily constant. The problem of varying velocities will be discussed later; for now velocity is assumed to be constant, but the term $\overline{v}$ will be used to ensure consistency with later results.

DETERMINING THE RAY PARAMETERS

Determining x_s, x_g, and t for a particular event on a particular trace is not difficult, because we can easily determine these values by looking at the trace header and by picking the travel time of that event. Determining p_s and p_g, its ray parameters, can be more difficult, however.

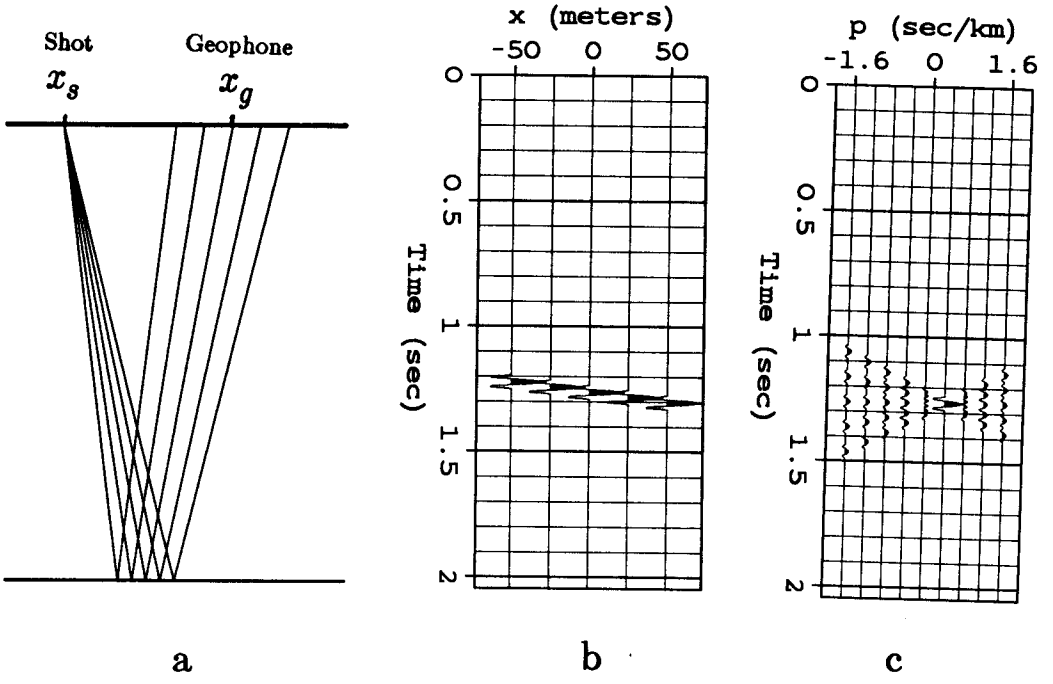

FIG. 2. Determining ray parameters. Figure 2a shows how a short-base common-shot gather might be collected in the field, while Figure 2b shows the possible results of this seismic experiment. Figure 2c shows the results of slant-stacking this data; from the slant-stack section we can determine p_g.

Typically, one determines p_s and p_g by performing slant stacks over small bases. For instance, Figure 2 shows how p_g might be determined. Several traces having shotpoints *at* x_s and receivers *near* x_g are gathered, and a slant stack is performed on these traces. The value of p that corresponds to the highest amplitude on the slant stack at a particular time t is picked, and this p is considered to be p_g. Similarly, several traces having shotpoints *near* x_s and receivers *at* x_g can be gathered and slant stacked, and a value of p picked at time t; this p corresponds to p_s. The two "summation bases", as the locations of these traces are known, are shown in Figure 3 in the form of a stacking chart.

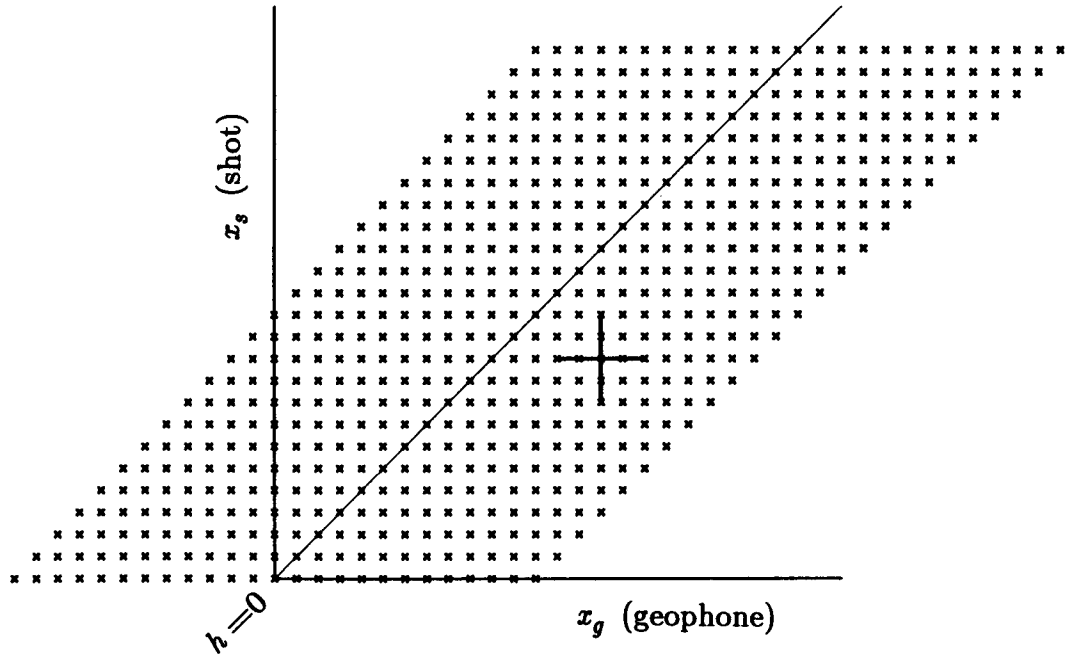

FIG. 3. A stacking chart showing "summation bases" that can be used to determine p_s and p_g. The heavy horizontal line denotes a short-base common-shot gather, whose traces can be used to determine p_g. The heavy vertical line denotes a short-base common-geophone gather, whose traces can be used to determine p_s.

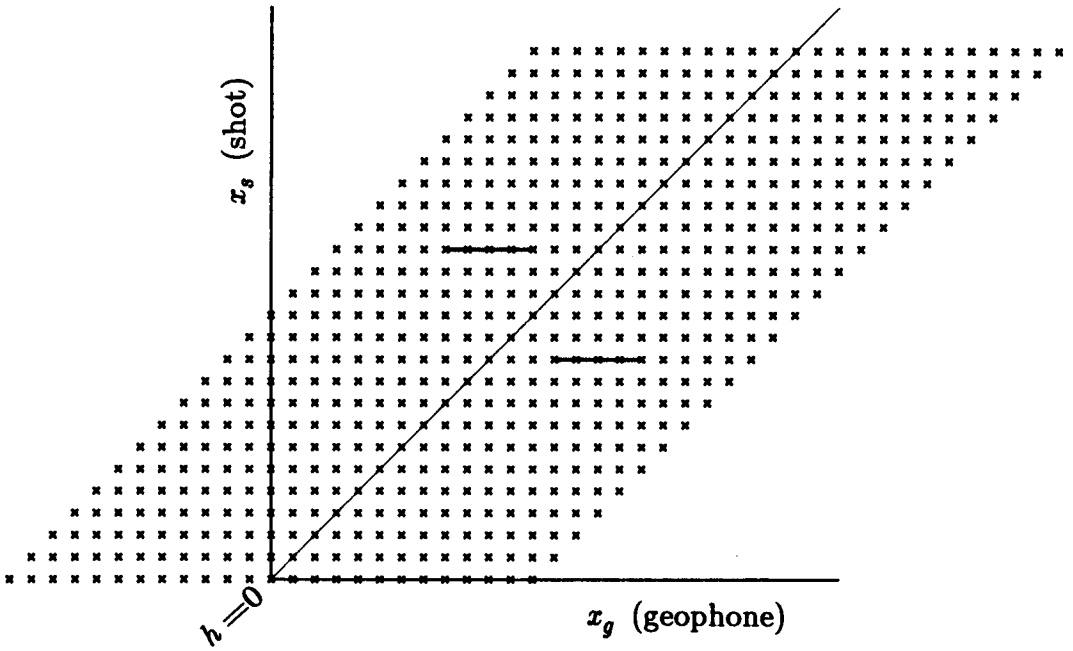

FIG. 4. A stacking chart showing a more traditional placement of the summation bases used to determine p_s and p_g. The heavy horizontal line to the right of the zero-offset line denotes a gather whose traces can be used to determine p_g, while the heavy horizontal line to the left of the zero-offset line denotes a gather whose traces can be used to determine p_s. Note that this works only in cases where the principle of reciprocity can be applied.

A more traditional way of picking p_s and p_g (in the Soviet Union, anyway) is shown, again in the form of a stacking chart, in Figure 4. In this method we use the principle of reciprocity: we determine x_s by placing a *shot* at x_g and slant-stacking the gather of traces from geophones near the point x_s. An advantage of this second method is that we are not thrown off by differences in the spacings between geophones and shots; a disadvantage is that a split-spread recording scheme must be used to gather the reciprocal data. Another disadvantage of this method is that it does not work well when we are interested in looking at converted waves; we should not blindly invoke reciprocity when the shot function and geophone response are not identical (e.g., when we have an explosive source and horizontal geophones).

There is an art to picking p_s, p_g, and t from slant-stacked gathers. Researchers in the Soviet Union have studied this problem for many years, and have successfully taught computers how to do the picking. I did not study that particular problem while I was in Moscow, so I won't try to discuss it here. (The synthetic data that I will present later in this paper had its values of t, p_s, and p_g picked by a computer at the Gubkin Institute in Moscow.) The rest of this paper is devoted to the problem of analyzing the data after the picking operation has been performed.

MIGRATION IF $\overline{v}$ IS ALREADY KNOWN

I will assume for the present discussion that $\overline{v}$ is known, and that it is constant. When this holds true, the travel-time equation for a point diffractor located at an arbitrary position (x_0, z_0) is:

$$\overline{v}^2 t^2 = \sqrt{(x_R - h)^2 + z_0^2} + \sqrt{(x_R + h)^2 + z_0^2} \quad . \tag{1}$$

(Recall from the above section on notation that x_R is the horizontal distance from the midpoint (y) of the observation system to the diffracting point, so $x_R = x_0 - y$.) When equation (1) is solved for z_0, we get

$$z_0^2 = \left(1 - \frac{4h^2}{\overline{v}^2 t^2}\right)\left(\frac{\overline{v}^2 t^2}{4} - x_R^2\right) \quad . \tag{2}$$

If we assume that h is known (it should be; h is simply half the distance between the shot and geophone), that $\overline{v}$ is known (this is the main assumption of this section), and that t has been picked and thus is also known, then we see that if we graph z_0 as a function of x_R, we obtain an ellipse (this figure is known, I believe, as an aplanat).

The significance of equation (2) is that it gives us some idea of the location of the reflecting point: the point must be located somewhere along the ellipse, if we have

picked the correct value for t and used it in equation (2). The problem now is to narrow down this location still further. A reasonable way to do this is to assume that our reflection didn't actually come from a reflecting point, but from a small tilted "dip bar", as was illustrated in Figure 1. Because the ellipse described in equation (2) would be tangent to the dip bar at the point of reflection, it follows that if we can determine the angle of dip of the dip bar, we can determine the location of the dip bar along the ellipse. Once we know the actual location of the dip bar, we can plot this little bar as a short line on a time section or a depth section; and by plotting all of the picked (p_s, p_g, t) data in the form of such bars, we can build up a picture of the subsurface reflectors.

It is necessary, then, to find the dip angle ϕ of the particular dip bar whose location we are attempting to find. We can make use of the fact that $\sin\theta_s = \overline{v}p_s$ and $\sin\theta_g = \overline{v}p_g$, with θ_s and θ_g being the angles of the downgoing and upcoming rays. We also recall that the angle of incidence onto the dip bar equals the angle of reflection from it, and with a little algebra we find that

$$\tan\phi = \frac{\overline{v}\left(p_s + p_g\right)}{\sqrt{1-\overline{v}^2 p_s^{\,2}} + \sqrt{1-\overline{v}^2 p_g^{\,2}}} \,. \tag{3}$$

Now that the dip angle ϕ has been determined, we need to determine at what point along the ellipse in equation (2) the dipping reflector is located. Equation (2) can be differentiated with respect to x_R, and we can make the substitution $dz_0/dx_R = -\tan\phi$ (the minus sign results from the fact that in our system of coordinates, z_0 *increases* with depth). Solving for x_R, we find

$$x_R = \frac{\dfrac{\overline{v}t}{2}\tan\phi}{\sqrt{1-\dfrac{4h^2}{\overline{v}^2t^2}+\tan^2\phi}} \,. \tag{4}$$

Because we know z_0 as a function of x_R from equation (2), we can make an appropriate substitution into equation (4) to obtain

$$z_0 = \frac{\dfrac{\overline{v}t}{2}\left(1-\dfrac{4h^2}{\overline{v}^2t^2}\right)}{\sqrt{1-\dfrac{4h^2}{\overline{v}^2t^2}+\tan^2\phi}} \,. \tag{5}$$

So now we have the equations that we wanted. Once p_s and p_g have been picked, we can use equation (3) to determine ϕ. And once ϕ is known and t has been picked, we can use equations (4) and (5) to determine x_R and z_0. Once x_R is known, it is trivial

to find x_0 (recall that $x_0 = x_R + y$).

This process, then, is a form of migration before stack. Using our values of x_0, z_0, and ϕ, we can produce a depth section, or we can produce a time section by converting from depth to time according to the formula

$$t_0 = \frac{2z_0}{\overline{v}} . \tag{6}$$

FINDING $\overline{v}$

Let us continue to assume that $\overline{v}$ is constant but unknown. All we know are the parameters that we picked (t, p_s, and p_g) and the half-offset h. It can be shown that when $\overline{v}$ is constant over the section,

$$\overline{v}^2 = \frac{1 - \frac{h}{t}(p_s - p_g)}{(p_s - p_g)\frac{t}{4h} + p_s p_g} . \tag{7}$$

I was able to obtain this result only after some rather messy algebra; I know of no easy way to derive it, but that doesn't mean that an easy way doesn't exist.

Equation (7) is accurate as long as $\overline{v}$ is constant, but in practice our determinations of p_s and p_g are sometimes inaccurate, and thus I introduce a new parameter, v_{CDR}: this parameter is defined to be the value of $\overline{v}$ that is found by use of equation (7). That is,

$$v_{CDR}^2 \equiv \frac{1 - \frac{h}{t}(p_s - p_g)}{(p_s - p_g)\frac{t}{4h} + p_s p_g} . \tag{8}$$

It is important to keep in mind the distinction between v_{CDR} and $\overline{v}$. The measured velocity, v_{CDR}, can vary greatly because of small inaccuracies in p_s or p_g, and thus it can vary sharply for different picks. In contrast, $\overline{v}$ is a smoothed (and possibly constant) velocity function. Thus, it would be a mistake to use v_{CDR}, once it has been determined, in place of $\overline{v}$ in equations (3), (4), and (5). If v_{CDR} were used, dip bars from the same reflector would most likely be mapped semi-randomly into various places in the final section instead of onto one smooth reflector, because each dip bar would be mapped according to its own velocity, the poorly-determined value v_{CDR}.

There are uses for v_{CDR}, however. The first is in the determination of $\overline{v}$. By looking at the values of v_{CDR} from a number of different picks, one can develop a smoothed

velocity function, $\overline{v}$. The velocity v_{CDR} can also be used as a measure of reliability of the pick. If v_{CDR} for a given dip bar differs greatly from that of its neighbors, it is reasonable to assume that that particular dip bar represents noise rather than a well-behaved signal, and the computer can accordingly decide if it should be plotted.

PROBLEMS OF NON-CONSTANT-VELOCITY DATA

CDR would not be very useful if it worked only when the velocity was constant. However, my derivations up to this point have been based on that assumption. Let us examine how to extend these derivations to the relatively simple case of $v = v(z)$. One difficulty is that my "average velocity", $\overline{v}$, has not been used in a consistent way. During some parts of the derivation I have treated it as v_{rms}, which produces approximately-correct travel-time curves as a function of offset, and which is defined by the equation:

$$v_{rms}^2(t_0) \equiv \frac{1}{t_0}\int_0^{t_0} v_{layer}^2(t)dt \ , \tag{9}$$

where $v_{layer}(t)$ is the true layer velocity as a function of vertical travel time. During other parts, I have treated $\overline{v}$ more as v_{avg}, which produces correct time-to-depth mapping for the case of horizontal reflectors and normal rays, and which is defined as:

$$v_{avg}(t_0) \equiv \frac{1}{t_0}\int_0^{t_0} v_{layer}(t)dt \ . \tag{10}$$

Thus, the exact meaning of $\overline{v}$ is not too clear. For a special case, though, the case in which reflectors are horizontal ($\phi = 0$ and $p_s = -p_g$), it can be shown that $\overline{v}$ found in equation (7) is equivalent to the v_{rms} defined in equation (9). When we combine equations (5) and (6) to find t_0, the $\overline{v}$ that appears in the combined equation is also equivalent to the v_{rms} defined in equation (9). Thus in some cases, $\overline{v}$ can be considered an analog of the traditional v_{rms}. This does not always hold true, though; if we use equation (5) by itself to find z_0, we will not get a correct answer, because v_{rms} is not accurate in doing time-to-depth conversions. And it is not clear what meaning $\overline{v}$ has when the reflector is not completely horizontal.

The fact is that equations (3), (4), (5), and (8) work in practice, as the examples in a later section will show. One possible explanation for this success is that as long as the velocity gradients are not too great, the various "average" velocities, such as v_{rms} and v_{avg}, are not much different from one another, and then it is possible to speak of $\overline{v}$ as

being a generalized average velocity. And, as we have seen, in some cases $\overline{v}$ acts consistently like v_{rms}. It appears that the reasoning behind my derivations might not be too inaccurate even when $\overline{v}$ is not constant, as long as it is not too variable.

Besides causing problems in the theory, variable velocities also cause some complications in processing. Many of these difficulties, such as analyzing velocities when the positions of the reflectors are not yet well-defined (we don't know exactly where the reflectors are until we know the velocity structure), are solved by use of an iterative algorithm. For instance, when migration is first performed on the data, an educated guess about the velocity function is used. From this migrated section it is possible to get a fairly good idea of how v_{CDR}, and thus $\overline{v}$, vary spatially. Then this new velocity function, $\overline{v}$, can be used to process the data.

Once an approximate velocity function has been found, equations (3), (4), (5), and (6) can be used. Because t_0 is not found until equation (6), and because $\overline{v}$ has been found as a function of t_0, an iteration to find the correct t_0 must then be performed. That is, equations (5) and (6) show how t_0 depends on $\overline{v}$ (and on other variables, some of which, such as ϕ, are also dependent on $\overline{v}$), but $\overline{v}$ in turn has been determined as a function of t_0 (and possibly y, depending on the exact velocity analysis algorithm that is being used). Thus an iterative process must be used to find t_0.

Once a reasonably good image has been obtained through the use of this approximate velocity function, one could presumably return to the velocity-analysis stage and fine-tune the velocity estimates, sharpening the image some more. I have not found it necessary to take the process this far, however, at least with the synthetic data that I have processed.

It should be noted that the velocity v_{CDR} associated with a particular dip bar need be determined only once. The difficulty in velocity analysis is determining where that dip bar should be located. We want velocity as a function of t_0 (and possibly y); until we apply equations (3), (4), and (5), we do not know the t_0 and y values that should be assigned to the dip bar and its associated v_{CDR}.

The CDR method, then, has some difficulties when velocity is not constant, because the theory (as I have developed it) is derived with the assumption of a constant-velocity medium. In practice, however, CDR seems to work well even when velocity variations are fairly sharp. Certainly the assumptions made in CDR processing are no more unjustified than the assumptions that go into the conventional "NMO plus stack plus migration" process.

FINE POINTS OF THE METHOD

Although I have stated the basic equations necessary for CDR migration, there are some fine points I have not yet covered. Most of these are of interest only if you are planning to write your own CDR program, and thus you may wish to skip the following five or six pages. But one fine point is necessary for an understanding of the plots that I shall soon be showing: the question of how amplitudes are dealt with.

Amplitudes and velocity filtering

When the parameters p_s, p_g, and t are picked, the amplitude, a, is also picked. This amplitude can then be used to determine how intensely the dip bar should be plotted. But recall that I noted in the section on finding $\overline{v}$ that v_{CDR} could be used to determine the likelihood that the dip bar represents an actual reflection. If the value of v_{CDR} is close to the expected value $\overline{v}$, then the data is probably reliable. If these values are not very close, then that particular dip bar might represent noise rather than signal. The reliability of the data can be quantified as shown below, and if the data proves to be unreliable, a can be reduced appropriately.

Let α represent the reliability, as defined in the following formula:

$$\alpha \equiv \frac{v_{CDR} - \overline{v}}{\overline{v}} . \tag{11}$$

Then we can let c_s be defined as the "sharpness" constant, and change amplitude according to the formula

$$a_{plot} = a \cdot e^{-c_s \alpha^2} , \tag{12}$$

where a is the picked amplitude and a_{plot} is the amplitude to be used in plotting. Clearly, the greater the value of c_s, the more sharply the amplitude is suppressed when v_{CDR} does not correspond with $\overline{v}$. In effect, this is a form of velocity filtering. A typical value (the one that I used in plotting) is $c_s = 10$.

Size and shape of dip bars

There are other fine points to the CDR method, including deciding how long to make the dip bars and how to treat variable velocities.

Determining the dip-bar length is fairly straightforward. In a paper that was translated by Sword (Zavalishin, 1981), Zavalishin showed that an appropriate length d would be

$$d = \sqrt{2 z_0 \lambda / \cos\phi} , \tag{13}$$

where λ is the wavelength of the source waveform. (This formula actually gives the size of the reflecting area on a reflector illuminated by a single ray.) In making my plots I did not compute λ; instead I varied its value by trial and error until I obtained a plot in which the dip bars weren't so long that they degraded resolution, and weren't so short that the section looked choppy. This value turned out to be 9 meters, which (for a velocity of 3000 meters per second) would correspond to a source waveform that was .003 seconds long. Such a short waveform is not physically likely, but it should be kept in mind that this value was for a model produced by ray-trace methods, which operate in the high-frequency (short waveform) limit.

Once the dip-bar length has been determined, an amplitude taper can be applied to each dip-bar when it is plotted. For my plots I used a simple triangle taper: the amplitude was zero at both ends of the dip bar and increased linearly to a maximum value at the center. It is also useful to convolve a signal onto the dip bar rather than to plot the bar as a dipping line of delta functions. This may easily be done by running the plot data through a bandpass filter before making the plot.

Velocity analysis

The issue of how to treat variable velocities, and more specifically, how to make use of the results of velocity analysis, is more complicated. In fact, you might want to skip this section on the first reading. If you want to write a program that carries out CDR, you might need to know this, but otherwise, it is not vital to your understanding.

Anyway, here goes. Consider how velocity analysis works in conventional (NMO + stack) processing. A common-midpoint gather is formed, and various velocity functions are applied until a best fit is found (the best velocity function is the one that maximizes the semblance). This best velocity function is used to apply normal moveout (NMO) to the common-midpoint gather, and the moved-out gather is stacked to form a single trace.

In CDR, several different approaches are possible; here is one that works on my synthetic data set (this approach was briefly sketched in a previous section, but I describe it now in excruciating detail). This approach, by the way, is somewhat different than the one used in the Soviet Union, because I never learned in exactly which coordinates they displayed their velocity analyses, and how exactly they used these analyses in the migration process. This section, then, does not necessarily represent the CDR method as practiced in the USSR.

To begin, an arbitrary velocity function is chosen (it is most convenient if it is chosen to be constant). The picked parameters (p_s, p_g, and t) and the arbitrary velocity function are used to form the equivalent of an unmigrated but moved-out stacked section in the following fashion. Once equations (3), (4), (5), and (6) have been evaluated, giving the coordinates (x_0 and t_0) of the dip bar on a a migrated section, a diffraction process can be applied to undo the effects of the migration without undoing the effects of moveout. The equations that apply this process are:

$$t_{mo} = \frac{t_0}{\cos\phi} \tag{14}$$

and

$$x_{mo} = x_0 - z_0 \cdot \tan\phi \,, \tag{15}$$

where x_{mo} and t_{mo} represent the apparent reflector position after NMO and DMO but before migration. Figure 5 shows graphically what we have done. This might seem like a strange way of going about things, migrating and then applying a zero-offset diffraction, but its advantage is it preserves both the NMO and the dip moveout (DMO) portions of the migration process (see Hale (1983) for an explanation of DMO).

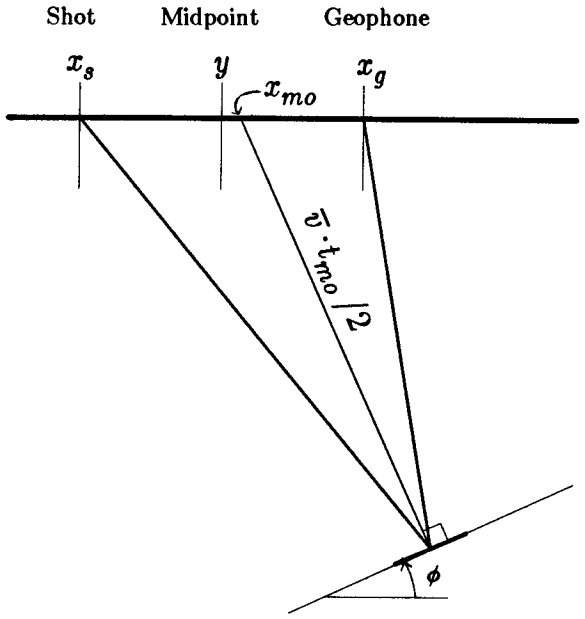

FIG. 5. Applying diffraction to a migrated dip bar. This figure shows how a simulated zero-offset reflection can be used to determine the apparent position of a dip bar after moveout but before migration. Once the values x_0, t_0, and ϕ have been found for a particular dip bar, it is not hard to determine what its apparent position (x_{mo} and t_{mo}) would be before migration. Note that x_{mo} is generally close to y.

Now we have associated each dip bar with a particular t_{mo} and x_{mo}, and each dip bar also has associated with it a particular value v_{CDR} which is obtained by use of equation (8). It is then relatively straightforward to form a velocity-analysis display showing v_{CDR} as a function of x_{mo} and t_{mo}. Despite the seeming complexity of this process, it is quite similar to what is done in conventional processing: moveout (both dip moveout and normal moveout) is applied, and the best velocity for a given time t_{mo} and midpoint position x_{mo} is picked.

Here we encounter one more level of confusion. I just pointed out that we can form a velocity-analysis display showing v_{CDR} as a function of x_{mo} and t_{mo}. We note, however, that x_{mo}, the unmigrated horizontal position, is probably close to y, the midpoint of the data-collection system (that is, halfway between source and receiver). This may not be obvious; Figure 5 will help make it clearer. It turns out that in later stages, it is not very useful to know velocity as a function of x_{mo}, while it is quite useful to know it as a function of y. Thus, we should analyze v_{CDR} as a function of y and t_{mo}, and smooth our results to form $\overline{v}(y, t_{mo})$.

Using the results of velocity analysis

Once we have produced a smoothed velocity function $\overline{v}(y, t_{mo})$, we apply it in the full migration process. One way of applying it, one that works, is to take our function $\overline{v}(y, t_{mo})$ and simply use it as $\overline{v}(y, t_0)$, recalling that t_0 is migrated travel time and y is the midpoint of the data-collection system. Although $t_{mo} = t_0$ only for flat reflectors (look again at Figure 5), this substitution (an incorrect one) produced better results than did continuing to use t_{mo} (at least on the synthetic data that I processed).

Let us assume that we have somehow come up with a velocity function $\overline{v}(y, t_0)$. (I don't know how this function is obtained in the Soviet Union; perhaps they use a more correct method than I have described above, or perhaps not. The rest of the techniques to be described are, at any rate, ones that have been tested at the Gubkin Institute.) Now we must perform some iterations. Taking our data picks (p_s, p_g, and t) at a particular midpoint y, we work through equations (3), (5), and (6) to find the value of t_0. (Because we are not yet interested in the value of x_R, we do not yet need to evaluate equation (4).) The value of $\overline{v}$ used in the first iteration was obtained simply by finding $\overline{v}(y, t)$. Because t is actual travel time rather than migrated or moved-out travel time, this value of $\overline{v}$ is not particularly accurate. After the first iteration, we have a preliminary value of t_0 that can be plugged into $\overline{v}(y, t_0)$. Then, using this new value of $\overline{v}$, we repeat the same process to get a better value of t_0. We can continue iterating until we

converge on the correct value of t_0. Now that we know t_0 and $\overline{v}$, we can evaluate equation (4) to find x_R, and the migration process is complete.

It might seem most obvious, and most physically realistic, for us to store $\overline{v}$ as a function of both t_0 and x_R, that is, as a function of both migrated travel time and migrated horizontal position. Then our iteration process would try to converge on values of both t_0 and x_R. However, this process is more expensive (we have to evaluate equation (4) at each step of the iteration) and less stable. I have tried various schemes, and the one described above, for all its flaws (the main one being the assumption that $t_0 = t_{mo}$), gave the best results when tried on my synthetic data.

Correcting the dip angle

There is one more fine point which may be even more obscure than the ones I have just discussed. The problem can be seen by looking at the diagram in Figure 6: when the velocity varies with depth, the tilt of the reflector will be calculated incorrectly, because of the curvature of the rays. Tests that I performed on my synthetic data set showed that the correction for this erroneous tilt was not especially helpful, and for some cases made the image worse. Thus, I prefer not to use it; but because it is used in the Soviet algorithm, I will describe it here.

It is convenient to assume that $\overline{v}$ is a function of t_0 (vertical travel time) only. Then we can describe the angle from vertical of a particular ray using the formula

$$\sin(\theta(t_0)) = v_{layer}(t_0) \cdot p \ , \tag{16}$$

where p is constant, and θ and v_{layer} are functions of depth (here depth is expressed in terms of vertical travel time, t_0). Thus the angle of a particular ray at any depth is known, as long as v_{layer} is known at that depth, and p, being constant, is known at all depths (at the surface, for instance). Then equation (3), which gives the angle ϕ of the dip of the reflector, can be rewritten as:

$$\tan\phi_{true} = \frac{v_{layer}(t_0)\left(p_s + p_g\right)}{\sqrt{1 - v_{layer}^2(t_0)p_s^2} + \sqrt{1 - v_{layer}^2(t_0)p_g^2}} \ , \tag{17}$$

where ϕ_{true} is the true dip angle of the reflector.

The question now is how to determine v_{layer} at a particular t_0. It is convenient to assume that $\overline{v}$ is equivalent to v_{rms}. As pointed out in a previous section, this assumption is correct for some, but certainly not all, cases. Looking back at equation (9), replacing v_{rms} with $\overline{v}$, and differentiating both sides with respect to t_0, we find that

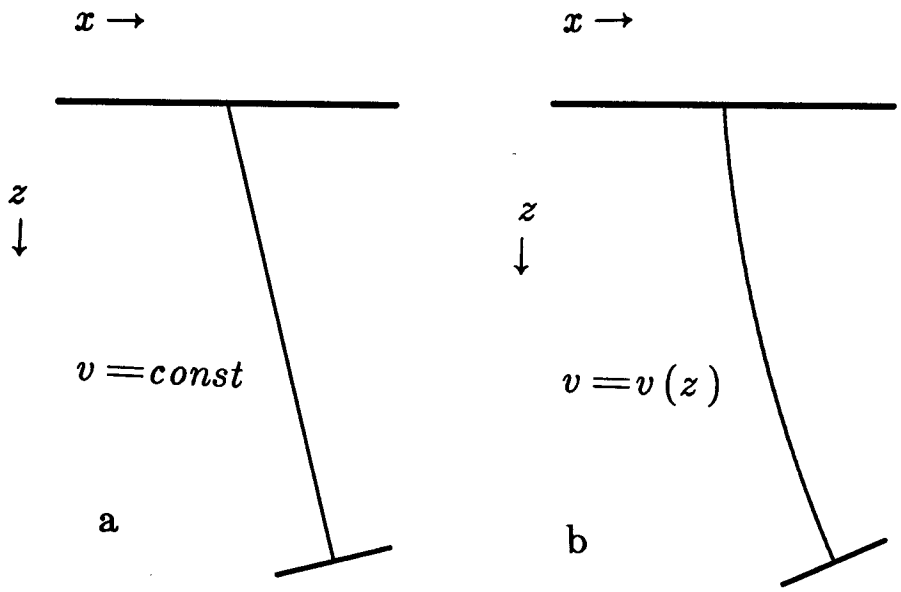

FIG. 6. How velocity variation can change the apparent dip of a reflector. Assume, for simplicity, a zero-offset case. Figure 6a shows an apparent dip that was determined using an average velocity value, while Figure 6b shows the true dip which, due to vertical velocity variations, differs from the apparent dip. Note the curvature of the ray in the latter case.

$$v_{layer}^2(t_0) = \frac{d}{dt_0}\left(t_0 \overline{v}^2(t_0)\right). \tag{18}$$

And so we can determine v_{layer} if we already know the velocity function $\overline{v}$. Once we have found v_{layer}, we can use equation (17) to find ϕ_{true}. And once we know ϕ_{true}, we can plot our section using the true dip angle.

As I noted previously, this correction actually seemed to degrade the quality of the image at some places in the synthetic examples on which I tested the method. I am not certain that this correction corresponds exactly to the correction used by the Soviets, although they are both based upon the same principles.

Time-to-depth conversion

Migrated time sections are the ones most commonly created, by use of equation (5) to find depth (z_0), and then the use of equation (6) to convert depth to vertical travel time (t_0). As noted in a previous section, this migrated time (t_0) is found in a way that is consistent with the idea that $\overline{v}$ corresponds to v_{rms}, at least for flat-lying reflectors. If equation (5) is used by itself, a migrated depth section can be created, but if $\overline{v}$ does correspond to v_{rms}, then the depths displayed will not be quite correct, because v_{avg} (see equation (10)), and not v_{rms}, should be used for time-depth conversions.

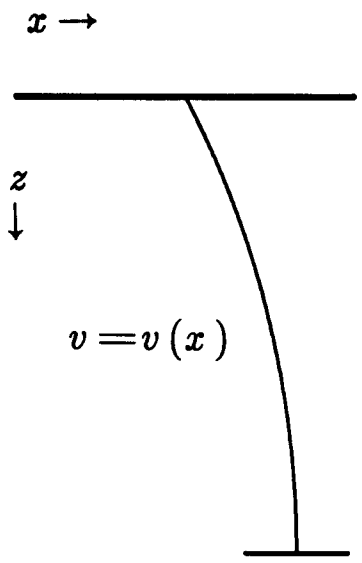

FIG. 7. Problems when velocity varies laterally. This figure shows how a zero-offset reflection from a flat reflector can result in a non-vertical ray at the surface when velocity varies laterally. This non-vertical ray can be mistakenly interpreted as coming from a dipping reflector.

There is an additional problem when velocity varies horizontally as well as vertically. This problem is illustrated in Figure 7, which shows how a normal ray from a flat reflector can end up traveling at an angle by the time it reaches the surface, and thus can appear to have come from a dipping reflector. Because of this problem, reflectors beneath horizontal velocity gradients appear fuzzy on depth sections. That is, even though the centers of the dip bars are positioned more or less correctly along the line of the reflector, each dip bar has the wrong dip, and the different bars do not reinforce each other. I have not yet tested methods of correcting this problem.

RESULTS PRODUCED WITH MODEL DATA

While I was in the Soviet Union, Boris Zavalishin of the Gubkin Institute developed the model shown in Figure 8. Dr. G. Matveenko of VNII Geofizika (another institute in Moscow) was kind enough to model this data using a program (based on ray tracing) that he had developed. The source was assumed to produce S waves and P waves of equal intensity, while the receivers were assumed to be vertical geophones. When the data is processed by conventional methods (NMO and stack, without migration), the result is as shown in Figure 9.

Figure 10 shows the result of stacking by CDR methods, but without migration, at a constant velocity of 3000 m/sec. This result was then fed into a velocity analysis

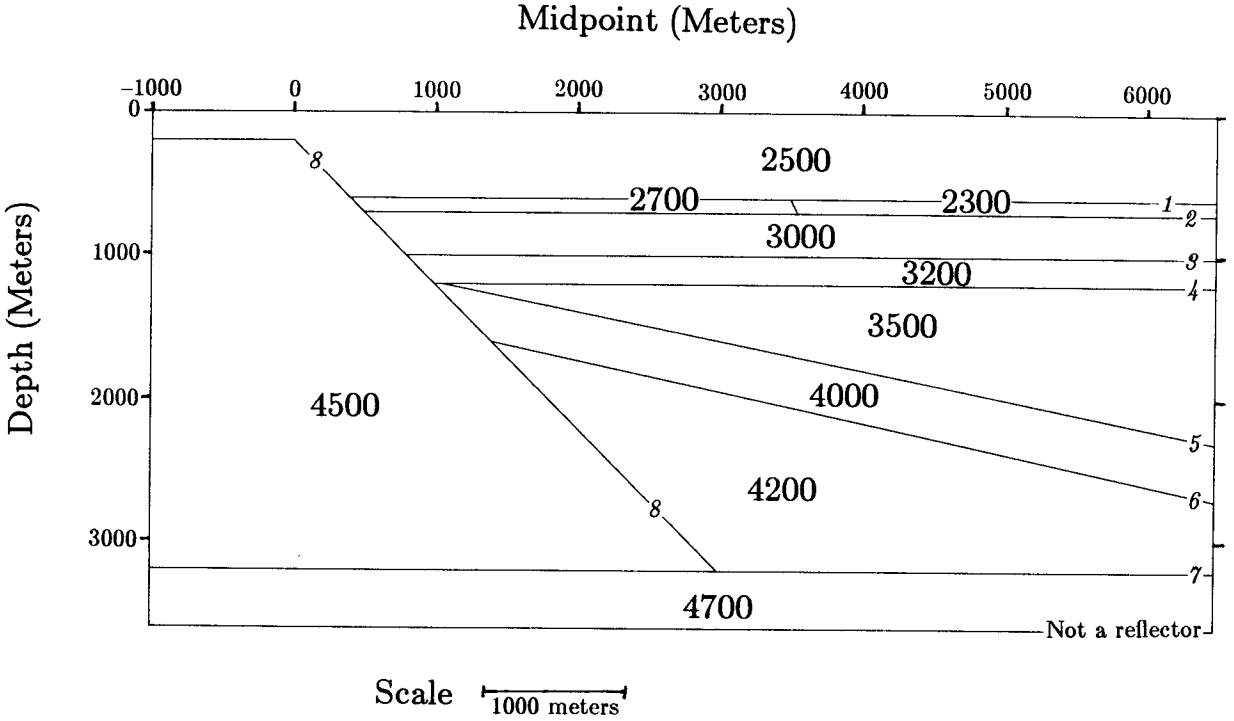

FIG. 8. Model used to generate the synthetic data shown in the following figures. P-wave velocity (v_P) is shown in m/sec; S-wave velocity (v_S) is always $v_P/1.732$. Each reflector is labelled with a number. The source produces S- and P-waves of equal intensity, while the receivers are vertical geophones. Distances between shots and between geophones are each 100 m. No vertical exaggeration has been applied.

program, which produced Figure 11; this figure shows the velocity analysis at a particular midpoint. Notice how well the peaks are defined. Figure 12 shows the result of a conventional (semblance) velocity analysis plotted in the same format.

With the results of the velocity analyses, Figure 13 was produced; it represents the migrated stacked section. Notice how much cleaner it is than Figure 12.

I produced Figure 14 by use of S-wave instead of P-wave velocities in order to obtain a shear-wave section. I computed the S-wave velocities by dividing the P-wave velocities by 1.732 (this ratio is the one that had been used to produce the model in the first place). Although much noise (here all unwanted reflections are considered to be noise) remains, the S-wave reflections clearly stand out. Figure 15 shows the results of using conventional processing to produce an unmigrated shear-wave section; the shear-wave events are almost completely hidden by noise.

It is not surprising that the CDR sections contain less noise than the conventional sections. Recall the sharpness constant (c_s) that was discussed previously; I used a value of $c_s = 10$ in the display of all of the CDR figures shown above. This constant

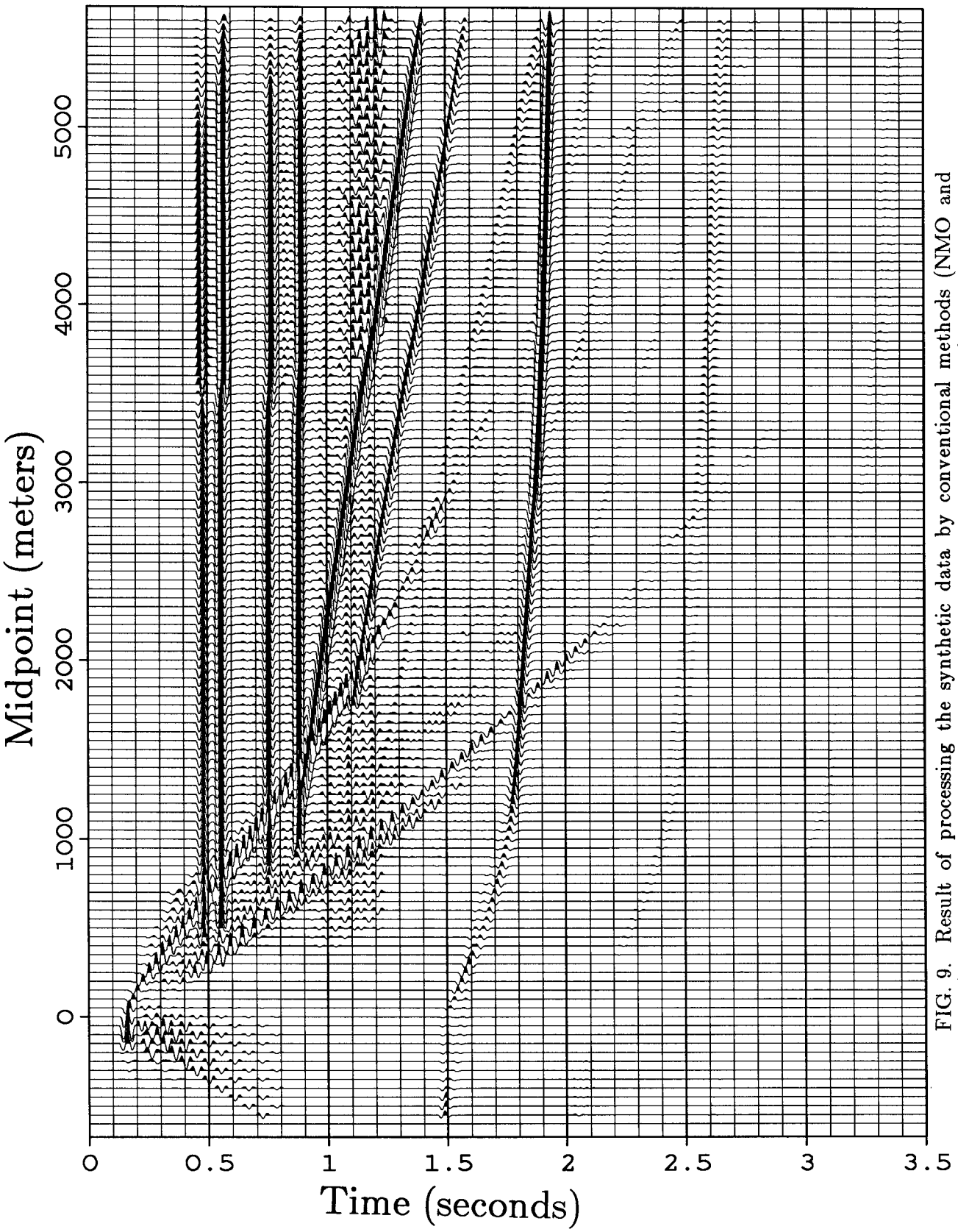

FIG. 9. Result of processing the synthetic data by conventional methods (NMO and stack). No migration has been applied. Note the converted waves and shear waves that produce "noise" on the section.

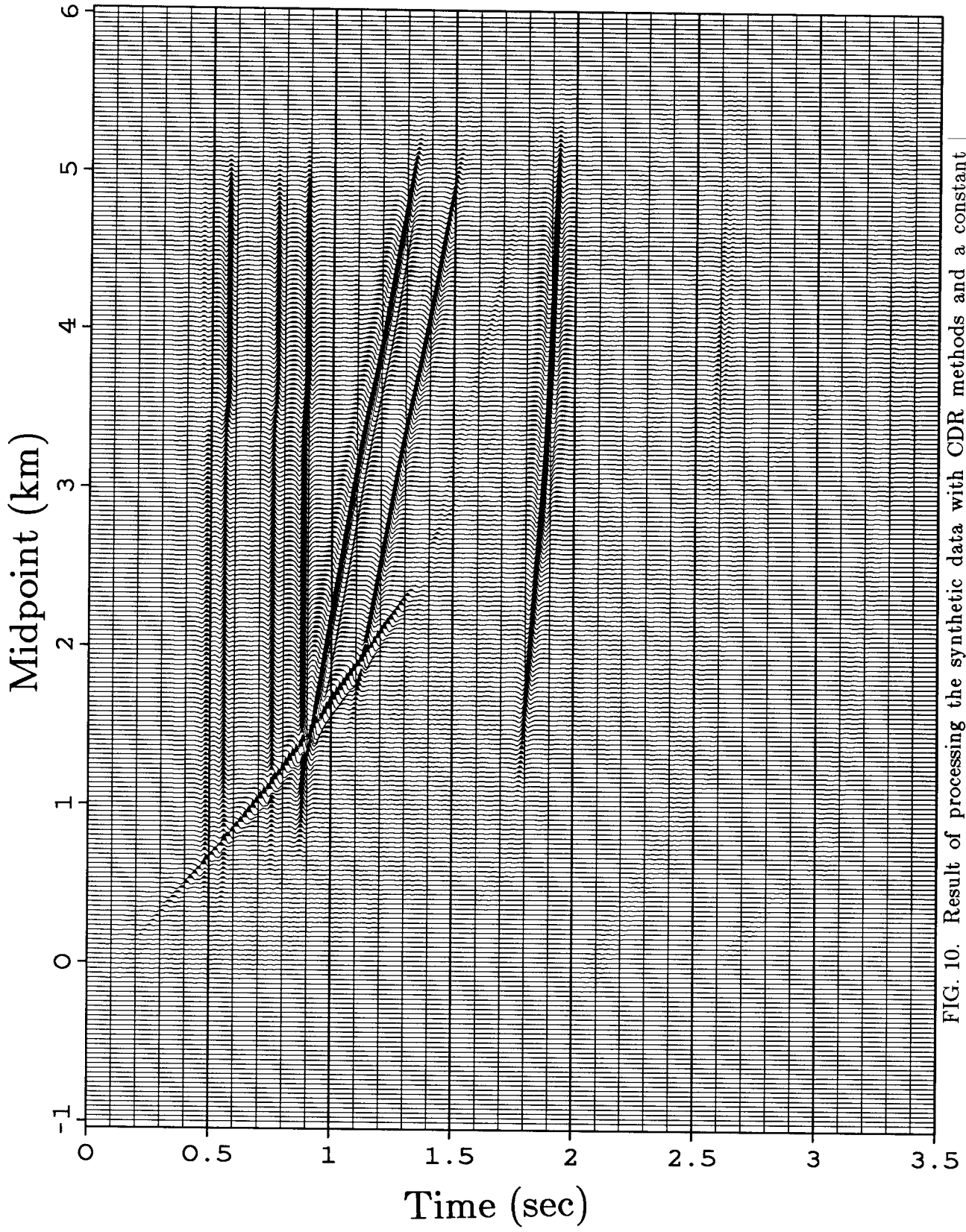

FIG. 10. Result of processing the synthetic data with CDR methods and a constant velocity of 3000 m/sec, with moveout but without migration. Data processed in this way can conveniently be used in velocity analyses, and the results of these analyses can be used in subsequent processing. A bandpass filter of 12–35 Hz has been applied to this plot.

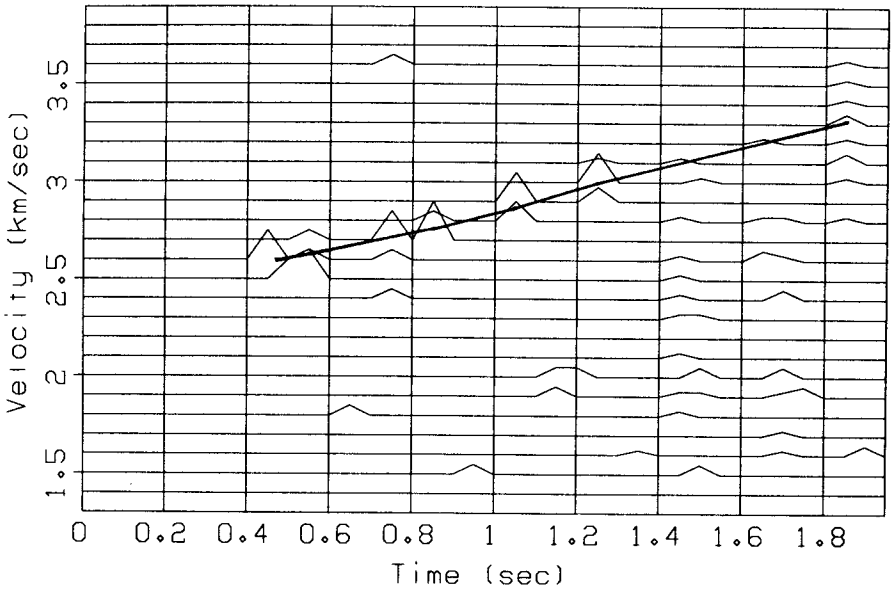

FIG. 11. The results of a CDR velocity analysis at the midpoint $y = 3000$ m. Note the sharpness of the peaks. The heavy line represents the picked velocity.

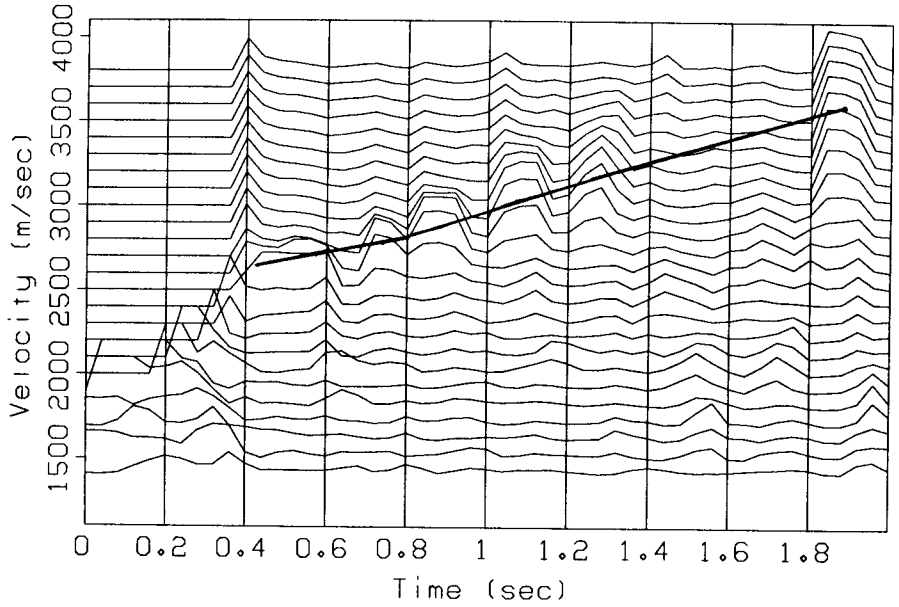

FIG. 12. The results of a conventional semblance velocity analysis at the same midpoint and in the same format as Figure 11.

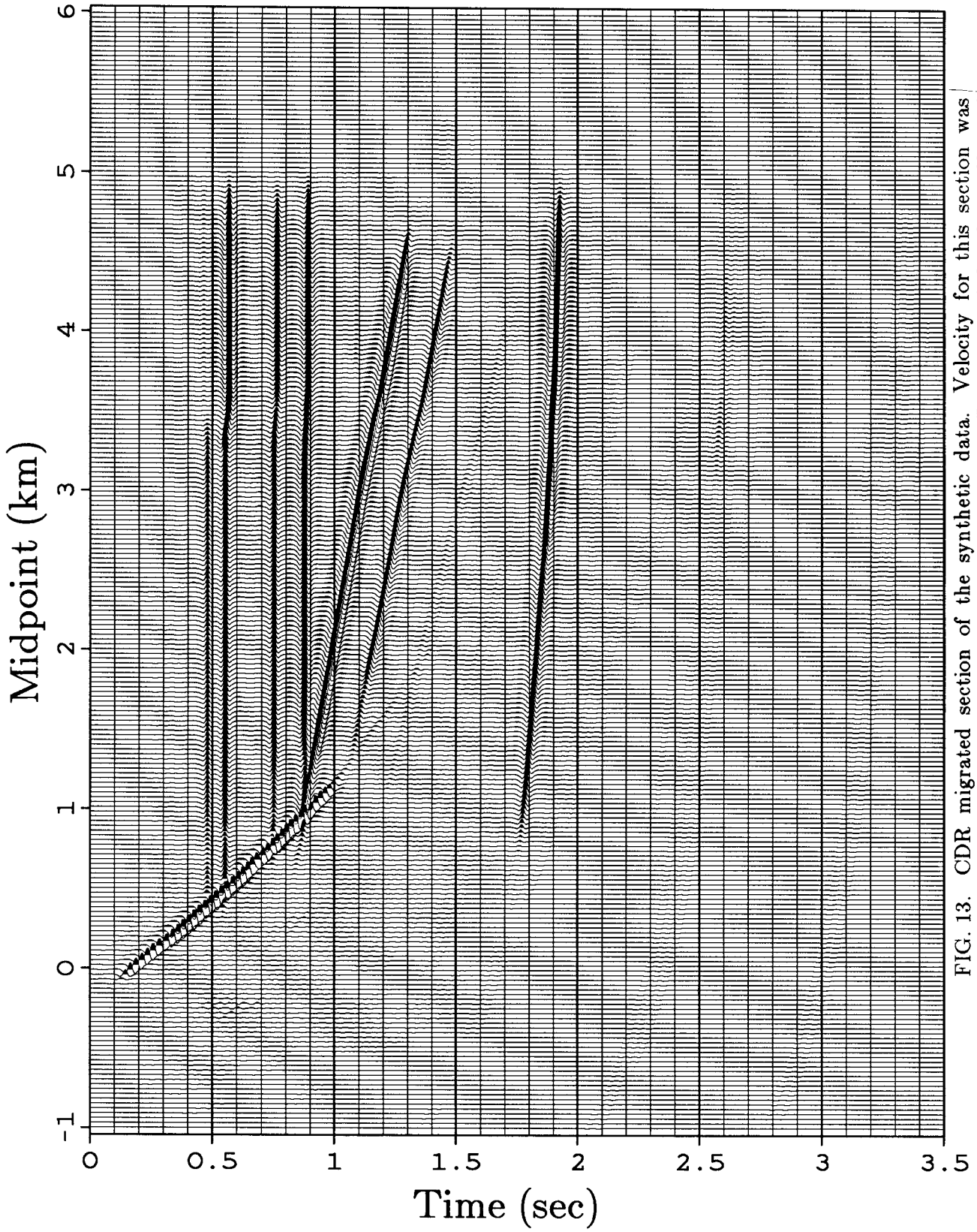

FIG. 13. CDR migrated section of the synthetic data. Velocity for this section was picked by use of velocity analyses similar to those in Figure 11. A bandpass filter of 12–35 Hz has been applied to this plot.

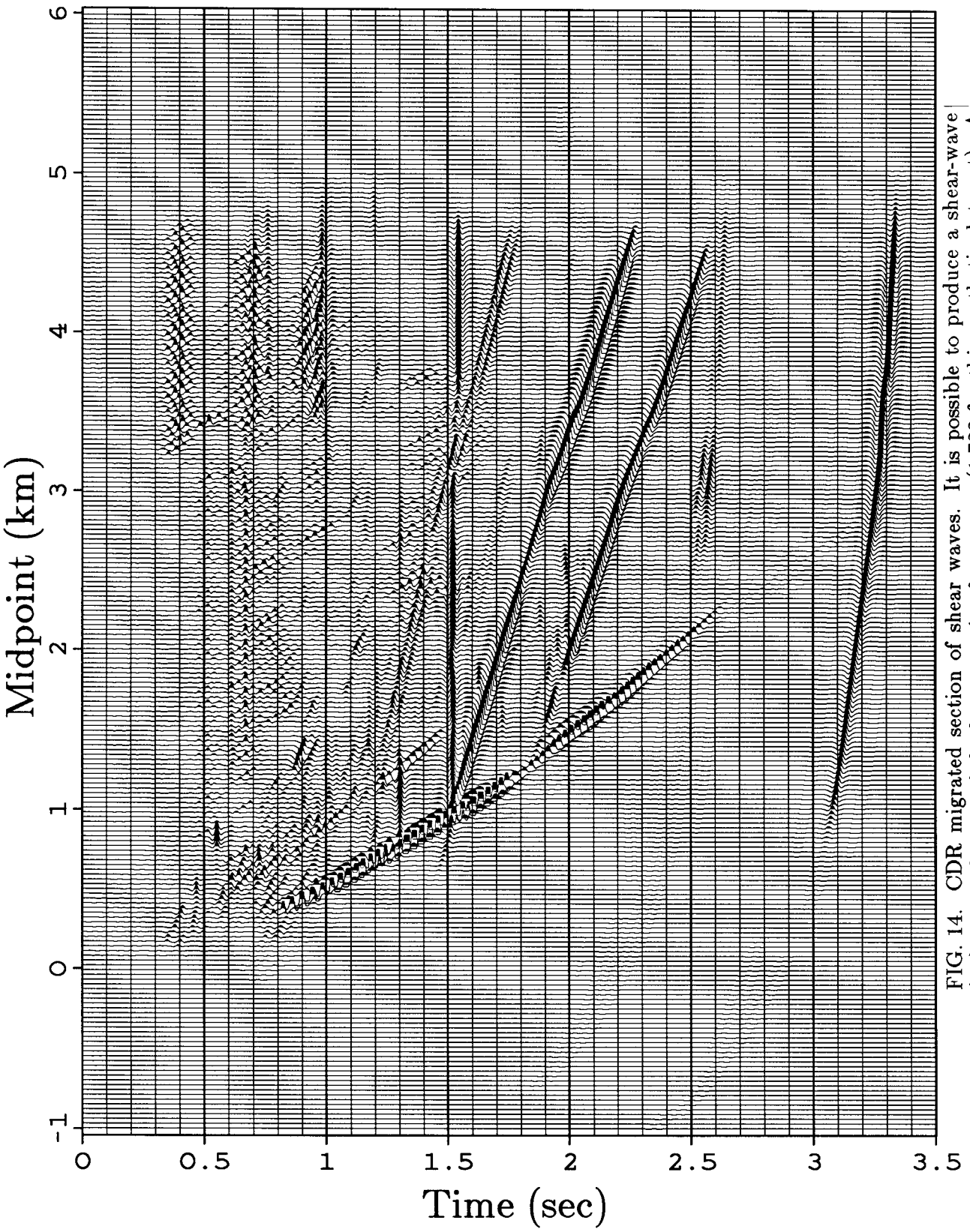

FIG. 14. CDR migrated section of shear waves. It is possible to produce a shear-wave (SS) section by use of the known ratio of v_P to v_S (1.732 for this synthetic data set). A bandpass filter of 12–35 Hz has been applied to this plot.

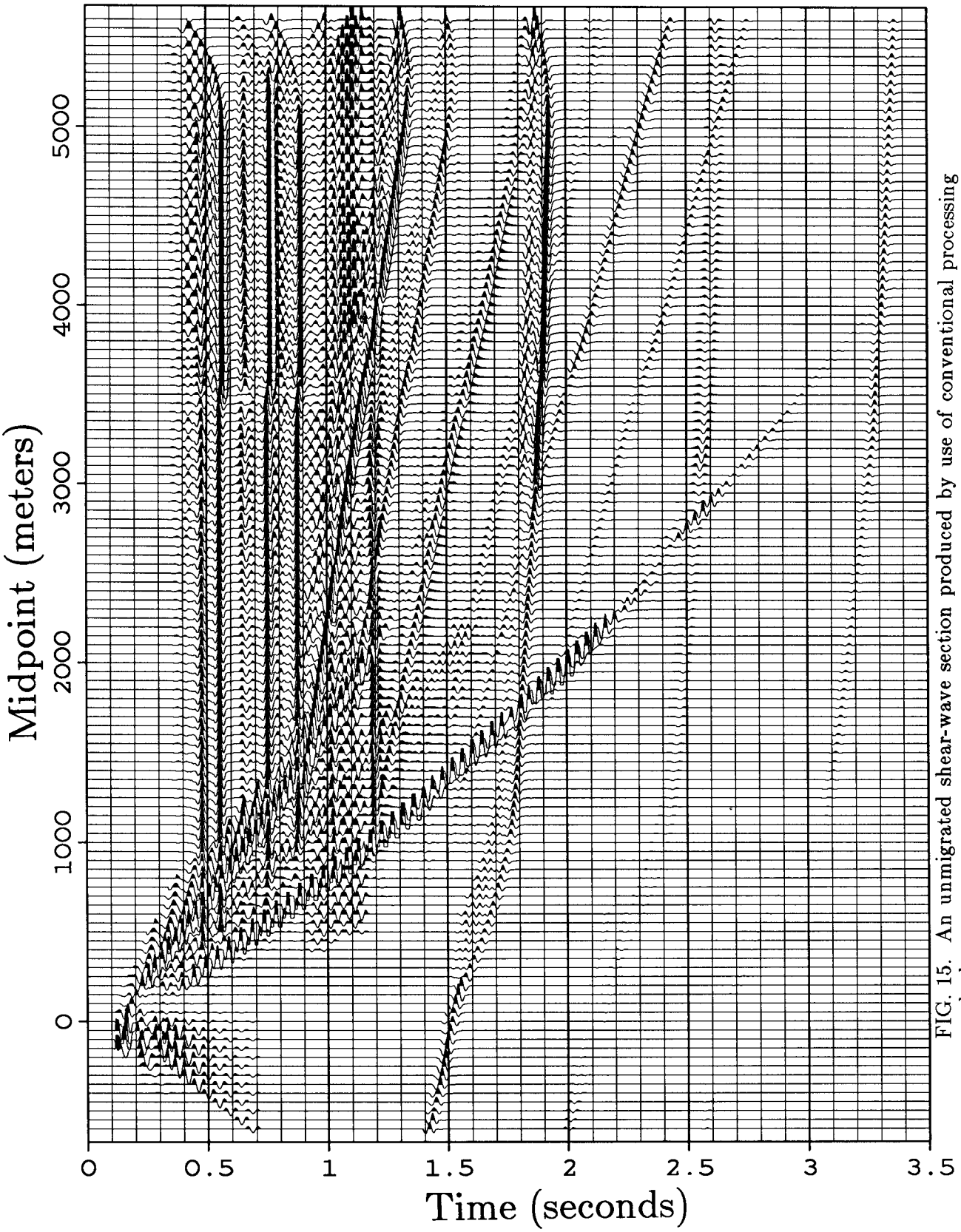

FIG. 15. An unmigrated shear-wave section produced by use of conventional processing methods.

represents a fairly strong velocity filter; many unwanted events were suppressed by this filter because they were produced by waves that traveled at incorrect velocities. The process of NMO plus stack also acts as a velocity filter, but a much weaker one.

CONCLUSIONS

CDR, used for many years on Soviet computers, works on US computers as well. There are advantages to the CDR method; we have just seen how effective the easily-implemented c_s velocity filter is. There are disadvantages as well; the main one, from an interpreter's point of view, is probably the loss of waveform information.

An advantage is that CDR processing uses very little computer time compared to almost any other migration method. The original picking of the data can be expensive, since all the data has to be slant stacked over short bases, but this picking can be done without any a priori assumptions about velocity, and all subsequent processing of the picked data is extremely cheap For example, the plotting program that produced the plots shown in this paper consumed more computer time than the migration program did. This speed suggests that the CDR method might be well-suited for interactive migration, where speed is more important than the exact reproduction of waveforms. Once the interactive CDR program has been used to find velocity, a more-expensive pre-stack migration process can be used to produce the final section. This procedure might be useful in regions of complex geologic structure. (Gray and Golden (1983) describes an iterative migration program based on principles similar to those of CDR.)

CDR produces very sharp velocity analyses, as Figure 11 shows. And recall that these analyses are already compensated for DMO, which means that correct velocities can be found even for events from dipping reflectors. Thus CDR may be a useful for producing velocity analyses, even if it is not subsequently used for imaging the section.

CDR's velocity-filtering characteristics may also prove useful; for this reason it could be an effective tool for finding and processing converted-wave reflections.

ACKNOWLEDGMENTS

Most of this paper is based on already-existing methods that were developed at the Gubkin Institute of Petrochemical and Gas Production in Moscow. I was fortunate to have the opportunity to spend nine months at the Gubkin Institute, where I studied these methods. Boris Zavalishin, who in many ways was responsible for my successful visit, was always most helpful, as was Evgeniy Varov, who with the aid of his computer programs was able to answer many of my questions about CDR. Dr. G. Matveenko of

VNII Geofizika developed and kindly ran the modeling program that generated my synthetic data, and Evgeniy Varov ran the programs that picked the ray parameters from this data. My visit to Moscow was made possible by the International Research and Exchange Board, which oversees, among other programs, an exchange of graduate students and young faculty members between the US and the USSR. Fannie Toldi proofread and edited this paper, but any mistakes are mine alone. And of course, I thank Jon Claerbout, who talked me into visiting the USSR, and the sponsors of the Stanford Exploration Project, whose contributions provided the the facilities for me to test my ideas upon my return to the US.

REFERENCES

Gray, W.C., and Golden, J.E., 1983, Velocity determination in a complex earth: Society of Exploration Geophysicists Expanded Abstracts with Biographies, 1983 Technical Program, 53rd Annual International SEG Meeting, Las Vegas, Nevada.

Hale, I.D., 1983, Dip-moveout by Fourier transform: Stanford University, Ph.D. thesis (also published as SEP-36).

Riabinkin, L.A., Napalkov, Yu. V., Znamenskiy, V.V., Voskresenskiy, Yu. N., and Rapoport, M.B., 1962, Teoriya i praktika seysmicheskogo metoda RNP (Theory and practice of the CDR seismic method): Trudy Moskovskogo Instituta Neftekhimicheskoy i Gazovoy Promyshlennosti im. Gubkina, v. 39, Gostoptekhizdat, Moscow (in Russian).

Rieber, F., 1936, A new reflection system with controlled directional sensitivity: Geophysics 1, pp. 97-106.

Sword, C., 1981, Controlled directional receptivity: a Russian method of pre-stack migration: SEP-26, pp. 289-296.

Zavalishin, B.R. (trans. by C. Sword), 1982, Improvements in constructing seismic images using CDR: SEP-30, pp. 63-76.

Zavalishin, B.R. (trans. by C. Sword), 1981, The size of the region that forms a reflected wave at a boundary: SEP-28, pp. 345-354.

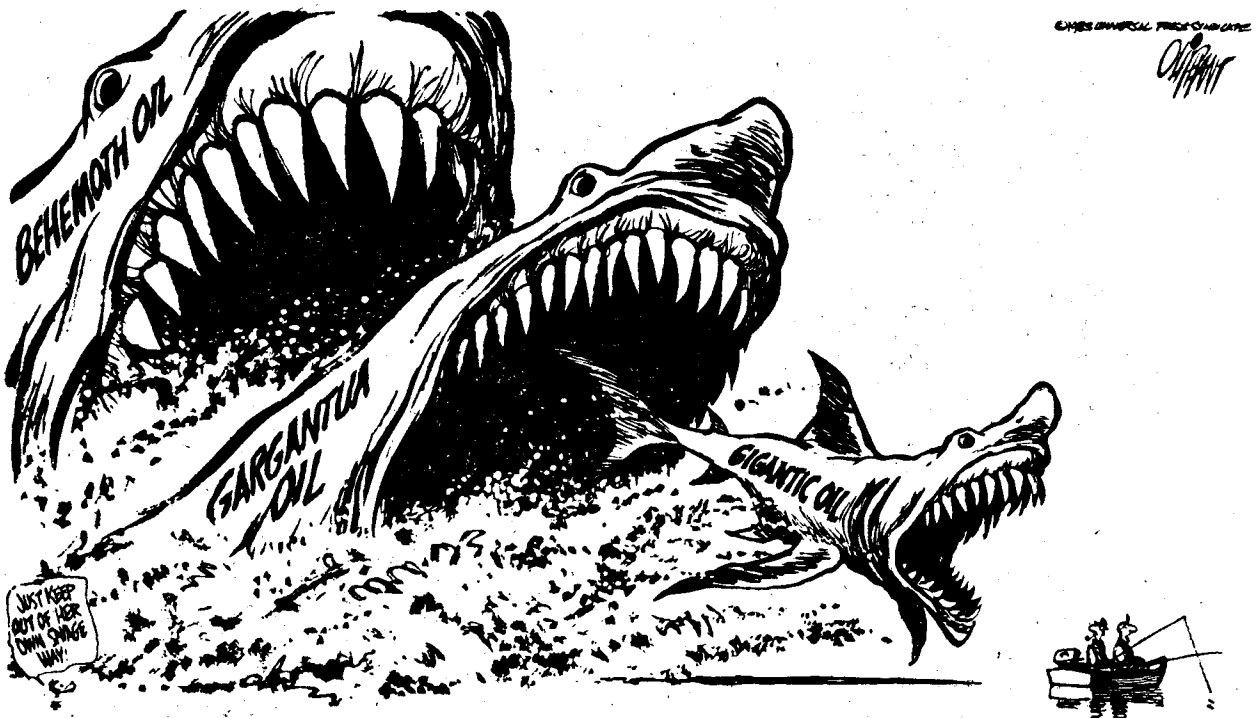

'AH, YES... NATURE IS BEAUTIFUL IN HER OWN SAVAGE WAY.'